Robust Imitation of a Few Demonstrations with a Backwards Model

Jung Yeon Park
Khoury College of Computer Sciences
Northeastern University
Boston, MA, USA
`park.jungy@northeastern.edu`

Lawson L.S. Wong
Khoury College of Computer Sciences
Northeastern University
Boston, MA, USA
`lsw@ccs.neu.edu`

Abstract

Behavior cloning of expert demonstrations can speed up learning optimal policies in a more sample-efficient way over reinforcement learning. However, the policy cannot extrapolate well to unseen states outside of the demonstration data, creating covariate shift (agent drifting away from demonstrations) and compounding errors. In this work, we tackle this issue by extending the region of attraction around the demonstrations so that the agent can learn how to get back onto the demonstrated trajectories if it veers off-course. We train a generative backwards dynamics model and generate short imagined trajectories from states in the demonstrations. By imitating both demonstrations and these model rollouts, the agent learns the demonstrated paths and how to get back onto these paths. With optimal or near-optimal demonstrations, the learned policy will be both optimal and robust to deviations, with a wider region of attraction. On continuous control domains, we evaluate the robustness when starting from different initial states unseen in the demonstration data. While both our method and other imitation learning baselines can successfully solve the tasks for initial states in the training distribution, our method exhibits considerably more robustness to different initial states.

1 Introduction

While reinforcement learning (RL) has shown remarkable success in many challenging domains [21, 38, 36], tasks with sparse rewards and long horizons still remain extremely difficult to solve. In such tasks, a positive reward is only encountered after the RL agent reaches the goal after a long sequence of actions, meaning that it cannot learn any useful signals until this occurs (typically the agent must reach the goal several times to learn reliably as well). Furthermore, the learning signal decreases exponentially with the horizon, which combined with slow gradient-based updates, can lead to catastrophic forgetting even after the agent learns to reach the goal.

Expert demonstrations can help RL agents solve difficult tasks [30, 43, 22]. These demonstrations can be used in the supervised setting where the agent imitates the expert's behavior, termed imitation learning (IL). However, naive behavior cloning (BC) of the expert's trajectories suffers from covariate shift: the agent's policy drifts away from the expert's, which leads to compounding errors due to RL's sequential nature. Furthermore, the distribution of states given in the demonstrations often has low-dimensional support with respect to the entire state space. As such, the agent cannot extrapolate correctly when outside of the demonstration data. Many approaches to solve this issue have been proposed [33, 39, 16], but such approaches require an interactive expert to query the correct actions.

Another way to use demonstrations is to combine imitation learning with reinforcement learning in a form of learning from demonstrations (LfD) [35, 13, 9]. In this case, demonstrations do not simply act as supervised labels and can guide the agent's exploration, and also act as augmentations to good
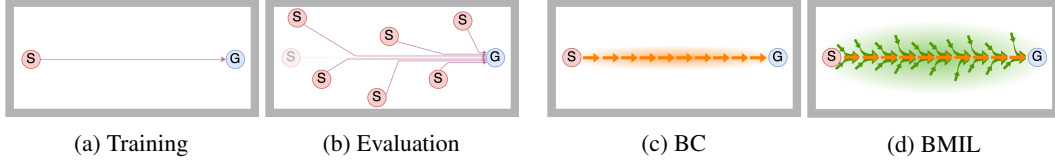
|(a) Training|(b) Evaluation|(c) BC|(d) BMIL|

Figure 1: **(a)**, **(b)**: Robustness: The policy is trained on a specified set of initial start and goal states and is evaluated at different start states. **(c)**, **(d)**: BMIL uses generated reverse-time rollouts from a backwards model (green arrows originating from the demonstration) to learn a wider region of attraction (green) around the demonstration data (orange) than BC.

data samples. These LfD approaches either use demonstrations to pretrain the policy [35, 9], use an auxiliary imitation loss in conjunction with the policy update [30, 22], or modify the reward function such that the agent is rewarded when it imitates the demonstrations [50, 31]. However, these methods require interactions with the environment whereas we do not assume such access in our setting.

One primary concern of relying on demonstrations is that they are costly to obtain, especially in real-world applications. Requiring an operator providing corrections in-the-loop to handle covariate shift is often prohibitive as well. Given only a few offline trajectories demonstrating successful task completion, an agent ought to be able to replicate the behavior from similar starting conditions, even if there are small perturbations along the way, and correct itself when necessary. We are primarily interested in this setting. In this work, we aim to minimize the number of demonstrations necessary for sparse-reward tasks, while preserving successful task completion. To tackle covariate shift, we seek an approach that will be *robust*, in the sense of Figures 1a and 1b: the agent is only trained with a few demonstrations from a single start state, but at evaluation time, it must generalize its behavior to a variety of unseen start states. If the agent can successfully complete the task from states adjacent to the demonstrated trajectory, then it can recover from small deviations from the demonstration.

Inspired by the notion of "funnels" in robotics [20] and feedback control [2, 19], we introduce a reverse-time generative model that can generate possible paths leading the agent back onto the demonstrations. These reverse rollouts provide useful information because every rollout ends within the support of the demonstration data. Assuming that the demonstrations lead to the goal, imitating these generated reverse rollouts and the original demonstration data allow the agent to reach the goal from more starting conditions, including unseen ones. As illustrated in Figures 1c and 1d, typical behavior-cloning (BC) methods focus learning on the small number of demonstrated states, whereas our proposed approach, Backwards Model-based Imitation Learning (BMIL), uses the reverse rollouts to learn a wider region of attraction around the demonstration. We validate our approach on a number of long-horizon, sparse-reward continuous-control tasks. Even from 5–20 demonstrations, BMIL provides a significant increase in the region of attraction and robustness on many domains compared to BC, or to using a forward dynamics model.

We summarize our contributions as follows:

- We propose an imitation learning method that pairs a backwards dynamics model with a policy and train on both demonstrations and imagined model rollouts.
- In the restrictive setting of an offline expert and no access to environment interactions, we show that a backwards model can improve robustness over behavior cloning.
- Our experiments on a variety of long-horizon, sparse-reward domains demonstrate that BMIL can noticeably extend the region of attraction around the demonstration data, even when trained on very small subsets of the state space.

2   Related Work

Imitation learning has a long history [27, 35] and is well-studied, as documented in various surveys [1, 25, 11]. The challenges of covariate shift and compounding errors are also well-known [27, 32]. Most solutions involve on-policy imitation learning, where environment interaction and interactive querying of the expert allow for the agent's distribution to match that of the expert [33, 39]. More closely related to our approach are methods that modify or augment the demonstrations to increase robustness. Laskey et al. [16] inject noise into the supervisor's policy during training to force the

demonstrator to provide corrections. Luo et al. [18] learn a dynamics model from demonstrations to conservatively extrapolate a value function that encourages the agent to return to the expert data distribution. Generative approaches have also been used in imitation learning [10, 46], but their focus is not on robustly following a few goal-reaching demonstrations.

Time-reversibility has been explored in RL, often as a form of regularization [41, 23, 49, 29, 34]. Reverse-time dynamics models, also called predecessor models, have also been used in RL [3, 6, 37, 15, 17, 48, 7]. However, in all cases, the reverse-time dynamics model is used as either an alternative to the forward-time dynamics model or as an auxiliary model in addition to the standard forward-time dynamics model, in order to mitigate model-compounding errors. The result is that the reverse-time dynamics model can accelerate RL and enable greater sample-efficiency. In this work, we take a different perspective where the reverse-time dynamics model is used to generate possible, unseen paths that can lead back to the expert demonstration and thus to the goal, thereby improving robustness in following the demonstration. Our work is also similar to [45], where a reverse-time dynamics model is used to generate possible trajectories; however, their focus is on offline RL, where the generated trajectories are used to connect distinct sets of states in the offline dataset.

3 Method

3.1 Preliminaries

We model the setting as a Markov Decision Process (MDP) with a continuous state space $\mathcal{S}$ and a continuous action space $\mathcal{A}$. $T : \mathcal{S} \times \mathcal{A} \mapsto \mathcal{S}$ is the transition function that defines the distributions of the next state $s_{t+1} \in \mathcal{S}$, given the current state $s_t \in \mathcal{S}$ and action $a_t \in \mathcal{A}$ taken at timestep t.

The objective of imitation learning is to learn a policy π_θ, parameterized by θ, that matches the expert's policy π_E. We assume that the expert generates demonstrations $\mathcal{D}_{demo}$ by rolling out its policy π_E in the environment. Note that we consider the more restrictive case of where demonstrations only consist of transitions (s, a, s') and not rewards, where s' is the next state.

Behavior cloning (BC) is a form of imitation learning where the policy π_θ learns to imitate expert actions via supervised learning. The policy learned by behavior cloning is found by minimizing the negative log-likelihood over the demonstration data

$$\mathcal{L}_{BC} = \mathbb{E}_{(s,a) \in \mathcal{D}_{demo}} \left[-\log \pi_\theta(a \mid s) \right].$$

Note that BC does not require environment interactions and can be considered to be offline. Furthermore, expert behavior is inferred only from demonstrations without access to the expert policy.

Compounding errors in behavior cloning As pointed out in [32, 44], behavior cloning suffers from covariate shift, where errors in the policy can compound and lead the agent to states where it cannot recover. Intuitively, this occurs as states in the training data $\mathcal{D}_{demo}$ is a small subset of the entire state space $\mathcal{S}$ and it is difficult for the policy π_θ to learn the optimal action for states outside of the training data. If during a rollout, once the policy π_θ makes an error and leaves the $\mathcal{D}_{demo}$, it may encounter completely new states, leading to the compounding of errors. Furthermore, as the agent moves farther away from $\mathcal{D}_{demo}$, there is very little hope for it to make the correct action and move back onto the distribution of the training data.

3.2 Problem Setting

We consider the same setting as BC, where we do not assume access to the environment or the expert policy during training, and only expert demonstrations without rewards are given. Furthermore, we assume that the expert demonstrations are given in the MDP where the sets of initial states S_0 and goals $\mathcal{G}$ are both very small subsets of the entire state space. An example of this scenario is a maze environment where the agent starts from the same initial state and tries to reach a fixed goal. Formally, we define the demonstration trajectories τ_{demo} as coming from a probability density

$$p(\tau_{demo} \mid \pi_E) = p(s_0) \prod_{t=0}^{T-1} \pi_E(s_t \mid a_t) p(s_{t+1} \mid s_t, a_t),$$

where $s_0 \in S_0$, and $s_T \in \mathcal{G}$. In our experiments, S_0 and $\mathcal{G}$ consist of a single start or goal state and/or the ε-ball of its neighborhood. As such, only a few demonstrations are required to learn a stable

optimal policy. Note that this is different from domains in previous work [30, 4] which consider random goal states, requiring many more demonstrations to learn optimal policies. We also assume that the expert policy is optimal in the sense that all demonstrations successfully reach a goal. While this is not strictly necessary in our method, our setting does not include rewards in τ_{demo} and thus we cannot discern whether demonstrations are optimal. This allows us to ignore the issue of modifying rewards as done in several offline RL algorithms [5, 14]. In order to use task completion success rates as an evaluation metric in our experiments, we consider only optimal demonstrations.

Our objective is to learn a policy that is robust to policy errors when imitating expert behavior and can learn to reach the goal from a variety of initial states. This is different than the multi-goal or multi-task setting, where the agent learns to solve multiple goals or tasks, usually from a small number of initial states. More formally, the robustness of the policy $R(\pi_\theta)$ is defined as

$$R(\pi_\theta) = \mathbb{E}_{s_0 \in S_R} \left[\mathbb{1}\{\exists t \leq T, s_t \in \mathcal{G}\} \right],$$

where the expectation is taken over S_R, where S_R is a strict superset of S_0. Note that our measure of robustness is somewhat coarse, in that we do not consider the shortest path to reach the goal from every start state (which would probably require more information such as diverse trajectories or environment interactions). Instead, we seek to extend the region of attraction around $\mathcal{D}_{demo}$ such that the learned policy can still reach the goal.

As we consider continuous states in our work, we measure the robustness R using samples from S_R, where we randomize either some or all of the state dimensions. For example, in robotic manipulation domains, we vary the position of the gripper as we are primarily concerned with being able to learn robustness from a variety of different starting positions. In other domains, we are interested in the policy's ability to recover from arbitrary initial states and so we vary not only the agent's starting position, but also the initial joint positions and velocities by adding uniformly random noise.

Throughout, we assume that there exists an action $a \in \mathcal{A}$ that allows the policy to go towards $\mathcal{D}_{demo}$ when in a state $s \notin \mathcal{D}_{demo}$. This scenario is true for many navigation and physics-based domains if we ignore rare circumstances such as irrecoverable unsafe states or the breakdown of the agent. We exclude such cases and assume that state transitions are reversible. We discuss some possible ways to incorporate irrecoverable states in Section 6.

3.3 Backwards Model-based Imitation Learning

In our work, we use a backwards dynamics model to provide more synthetic training data to the policy and therefore increase the policy's robustness. We call our method backwards model-based imitation learning or BMIL.

Backwards model The backwards model is a probabilistic generative model defined as $B = p(s_t, a_t \mid s_{t+1})$. This model estimates the conditional distribution of the reverse time dynamics. It takes in the next state and outputs the previous state and previous action. As we consider only continuous state and action spaces, we implement B as a conditional Gaussian, parameterized by ϕ.

The backwards model is decomposed into two functions $B = B_A \cdot B_S = p(a_t \mid s_{t+1}) \cdot p(s_t \mid a_t, s_{t+1})$, an action generator and previous state generator. The action generator B_A predicts which action was taken in order to land in the next state. There may be several such actions from different states that can lead to the next state. Thus the action generator implicitly encodes a backwards policy. It is important for this backwards policy to closely match the learned forward policy π but be different enough to generate diverse new rollouts for the policy to train on. The previous state generator B_S predicts the previous state given the next state and previous action taken. The goal of this generator is to accurately predict the backwards dynamics.

As we consider the setting with no access to the expert or the environment, B is trained only on $\mathcal{D}_{demo}$. The action generator and previous state generator are jointly trained by maximum likelihood

$$\mathcal{L}_B = \sum_{t=0}^{T} \log p(a_t \mid s_{t+1}) + \log p(s_t \mid a_t, s_{t+1}), \tag{1}$$

where s_t, a_t, s_{t+1} is the state, action, and next state, respectively, at timestep t.

Model rollouts Given expert demonstrations τ_{demo}, we use the backwards model to generate possible several short reverse rollouts or traces τ_B, starting from every state in τ_{demo}. As all of these

---

Algorithm 1 Backwards Model-based Imitation Learning (BMIL)

1: **for** N epochs **do**
2:     Train backwards model parameters ϕ using Eqn. (1).
3:     Generate K model traces τ_B from every state $s \in \mathcal{D}_{demo}$ and store them in $\mathcal{D}_M$.
4:     **for** M steps **do**
5:         Sample mini-batch of (s, a) from $\mathcal{D}_{demo}$ and $\mathcal{D}_M$ at a fixed ratio.
6:         Update policy parameters θ using Eqn. (2).
7:     **end for**
8: **end for**

---

traces end on states within the demonstration data $s \in \mathcal{D}_{demo}$ and as all demonstrations reach the goal, following these traces will eventually lead to the goal. For all $s_1, \ldots, s_T$ in τ_{demo}, we generate K traces τ_B in a time-reversed manner, where we start from the last state action pair $(s_H, a_H) \in \mathcal{D}_{demo}$ and then predict (s_t, a_t) for timesteps $t = H - 1, \ldots, 1$. These traces are collected into a buffer $\mathcal{D}_M$. As we assumed that there are no irrecoverable states in our setting, the rollouts reflect possible paths that the agent could have taken to reach $s \in \mathcal{D}_{demo}$. If the reverse time model B is accurate and the previous action generator B_A gives sufficiently diverse actions, the traces τ_B are then samples from the region of attraction or "funnels" around every state along the demonstration. As we assume all demonstrations reach the goal, these samples from the funnels can be used to learn a robust policy π_θ, as it can follow the traces onto the optimal path.

Action selection strategy for B_A As the backwards model B is trained only on a limited number of expert demonstrations, it is likely that B can only learn accurate reverse-time dynamics for states contained within or close to the demonstration data $\mathcal{D}_{demo}$ [47]. Thus repeatedly rolling out B_A would only generate traces whose state-action pairs are contained within $\mathcal{D}_{demo}$ and would not help with learning robust policies. However, we would like to generate diverse traces with new unseen state-action pairs in order to robustify the policy. To balance the model misprediction accuracy with generating plausible state-action pairs, we perturb only the first action generated from B_A and not the subsequent actions and also use short horizon lengths for the traces. Note that we are essentially choosing a good action selection strategy for B_A. Let a_E be the action that the expert would take. A good action selection strategy would place more probability mass closer to the support of the $\mathcal{D}_{demo}$, providing a "cover" of $p(a_E | s)$ but with a wider tail to provide diverse rollouts. As our backwards model B is probabilistic (implemented as a conditional Gaussian with diagonal covariance), we can easily perturb $p(a_E | s)$ by increasing the distribution's variance.

Let $a \sim \mathcal{N}(\mu, \sigma^2)$ be the previous action output by B_A. We consider two ways to generate action a: 1) simple scaling of σ and 2) resampling a new action a' by adding uniform noise, $a' = a + k, k = \mathcal{U}[-b, b]$, where b is a fixed hyperparameter. For the scaling strategy, we further scale σ by the entropy of the probability density as we wish to make the distribution "wider" for peaker distributions.

Algorithm   Our method BMIL is outlined in Algorithm 1. Given expert demonstrations with tuples of the form (s_t, a_t, s_{t+1}), we train the backwards model using Eqn. 1 to estimate the reverse-time dynamics $p(s_t, a_t | s_{t+1})$. We train our policy π_θ on both the demonstration data $\mathcal{D}_{demo}$ and the model traces τ_B by sampling from both at a fixed ratio and using maximum likelihood,

$$\mathcal{L} = p_d \mathcal{L}_{BC} + (1 - p_d)\mathbb{E}_{(s,a) \sim \tau_B}\left[-\log \pi_\theta(a \mid s)\right], \tag{2}$$

where p_d is the probability of sampling from $\mathcal{D}_{demo}$. As our aim is to learn a robust policy while still succeeding at the original start states and goals, we sample from the demonstrations at a higher ratio than the model traces. Note that BMIL does not depend on the type of imitation learning policy. Any algorithm can be used as long as the policy can be trained with samples of the form (s, a).

4   Experiment Design

4.1   Environments

We validate our approach on several continuous control domains: 1) the Fetch robotics environment [26], 2) maze navigation with two different agents, and 3) Adroit hand manipulation [30]. Figure 2 shows sample images of some environments. For the Fetch robotics environments, we consider the
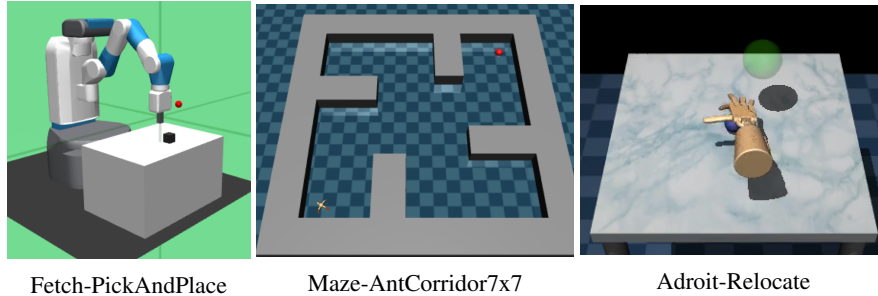
| Fetch-PickAndPlace | Maze-AntCorridor7x7 | Adroit-Relocate |

Figure 2: Sample images of some considered environments.

"Push" and "PickAndPlace" tasks where the objective is to control a Fetch end effector to either push an object to the goal or pick an object and place it at the target location. For the maze environments, we consider 3 mazes of increasing difficulty, where an agent must learn to move itself and then reach the goal. We use both a simple point and a 29-DoF ant agent. For the Adroit environment, we use the 'Relocate' task, where one must control a 24-DoF Adroit hand to pick up a ball and move it to a target location. All domains use the MuJoCo simulator [42] for a total of 9 distinct domains. All environments have sparse reward structures, where either every step has a constant negative reward until the goal is reached (Fetch) or only the goal has a non-zero reward (Maze, Adroit). In particular, the Maze and Adroit environments are quite challenging as they both consist of controlling the agent's joints to perform locomotion (maze) or dexterous manipulation (Adroit) over a long horizon. More detailed descriptions of each environment including its observation space are provided in Appendix A.

4.2 Demonstrations and Implementation Details

To generate demonstrations in the Fetch and Maze domains, we train an expert policy by adding the goal position to the state, as in goal-oriented learning, and use off-the-shelf RL algorithms [28, 8]. For the Adroit domain, we use a pre-trained policy from [30]. We use 5 demonstrations on the Push task and 10 on the PickAndPlace task, and 20 demonstrations for all Maze and Adroit environments.

For the policy, we use neural networks with 3 fully connected hidden layers with 256 neurons and ReLU activations. For the backwards model, we use 4-layer MLPs with 256 hidden units for both the action predictor B_A and previous state predictor B_S and use diagonal Gaussian distributions. To train the policy, we use $p_d = 0.5$ for the Fetch environments, $p_d = 0.8 \sim 0.95$ for the Maze environments, and $p_d = 0.8$ for the Adroit environments. We find that higher ratios are necessary for longer-horizon and more complex domains. For the model rollouts, we use the variance scaling action selection strategy for the first action only and use increasing rollout lengths for all domains, similar to [12]. For a more detailed discussion of experiment details, see Appendix B. Our code for the modified environments, generating expert policies, and running all experiments are available at `https://github.com/jypark0/bmil`.

4.3 Evaluation

We evaluate BMIL against behavior cloning (BC) and VINS [18]. VINS specifically aims to learn value functions robust to perturbations using negative sampling and the induced policy learns self-corrective behavior. VINS was chosen as it is most relevant to our setting; other methods such as DART [16] or SQIL [31] require either an online expert or environment interactions.

We use the same number of demonstrations for all methods and also keep the same policy network architecture and the total number of policy gradient steps equal across all methods. We train both the policy and backwards model until the backwards model loss converges. Note that our goal is not to solve the training task faster but rather to robustify the policy using the backwards model. Additionally, we wish to solve the task at various starting conditions while still being able to succeed at the original initial start-goal states.

To evaluate the robustness of the learned policy, we vary the initial states and compute task success rates. For Fetch, we fix the initial gripper, object, and goal position during training and vary the gripper's x and y position within the table boundaries during evaluation. We use 10,000 samples

			Robustness (%)			Relative to BC		
			BC	VINS	BMIL	BC	VINS	BMIL
FETCH	Push (5 demos)		$12.1_{\pm 0.3}$	$12.8_{\pm 0.4}$	$\mathbf{14.6}_{\pm 0.6}$	1	1.06	**1.21**
	PickAndPlace (10 demos)		$4.1_{\pm 0.1}$	$3.4_{\pm 0.1}$	$\mathbf{17.5}_{\pm 0.9}$	1	0.84	**4.31**
MAZE	Point (20 demos)	UMaze	$\mathbf{49.0}_{\pm 1.9}$	$39.5_{\pm 2.1}$	$47.8_{\pm 3.5}$	**1**	0.81	0.98
		Room5x11	$36.8_{\pm 3.4}$	$17.3_{\pm 2.8}$	$\mathbf{38.6}_{\pm 3.4}$	1	0.47	**1.05**
		Corridor7x7	$33.7_{\pm 1.5}$	$\mathbf{37.7}_{\pm 1.2}$	$\mathbf{38.9}_{\pm 2.3}$	1	**1.12**	**1.16**
	Ant (20 demos)	UMaze	$63.0_{\pm 1.0}$	$44.7_{\pm 2.1}$	$\mathbf{64.8}_{\pm 1.5}$	**1**	0.71	**1.03**
		Room5x11	$\mathbf{33.2}_{\pm 0.9}$	$30.2_{\pm 0.8}$	$29.1_{\pm 0.8}$	**1**	0.91	0.87
		Corridor7x7	$\mathbf{21.7}_{\pm 0.6}$	$19.6_{\pm 0.6}$	$17.6_{\pm 0.5}$	**1**	0.90	0.81
ADROIT	Relocate (20 demos)		$7.9_{\pm 0.7}$	$3.8_{\pm 0.7}$	$\mathbf{13.3}_{\pm 1.0}$	1	0.48	**1.68**

Table 1: Robustness evaluation for Fetch, Maze, and Adroit environments over 400, 100, 100 trials, respectively. The bounds indicate 95% confidence intervals. BMIL improves robustness considerably over BC in most environments.

during evaluation. For Maze, we initialize the agent to a random start position within a discretized grid of the maze and also add random uniform noise to the agent joints' `qpos,qvel`. We sample 100 initial states for each discrete grid cell and compute the success rate. Sampling points for each grid cell gives us an idea of which positions are easy for the agent to reach the goal. Intuitively, such positions would be those near the goal and the demonstrated path. For Adroit, we generate 1,000 random initial states by adding uniform noise to the `qpos` of the hand.

5   Results

Our experiments aim to answer the following questions: 1) how robust of a policy does BMIL learn? and 2) what components of BMIL are important to improve robustness?

5.1   Robustness evaluation

The robustness results are shown in Table 1. We note that the absolute robustness percentages are generally low for all methods because of the difficulty in extrapolating from limited demonstrations $(5 - 20)$ with a single pair of initial start and goal states. We therefore also include the relative improvement over BC.

In the Fetch environments, BMIL substantially increases robustness over BC and VINS. In particular, our method has an approximately 20% and 330% improvement over BC on Push and PickAndPlace, respectively. VINS on the other hand performs similarly to BC. We see a similar pattern on the harder Adroit environment, where BMIL improves robustness over BC by 68%. For the Maze environments, BMIL generally outperforms BC for the Point agent, while the robustness is decreased for the Ant agent. Somewhat surprisingly, BC performs quite well on the long-horizon Maze domains. It may be that BC has some built-in extrapolation capabilities or that the backwards model may need better latent representations with more powerful networks.

Empirically, we can see that having short reverse rollouts from the backwards model and using only slight perturbations still helps to increase robustness, even though the traces contain some model misprediction errors. We hypothesize that these traces do not necessarily need to be accurate in order to benefit the policy and simply need to be plausible paths that lead to the demonstrations. It may be that having the general correct direction contained in the traces is sufficient for the policy to eventually reach states in the demonstration data.

The success rates during training are shown in Table 5 in Appendix C.1. BMIL achieves success rates close to 1 for most domains, suggesting that increased robustness does not necessarily come at the cost of decreased performance on demonstrated start-goal states. On the other hand, VINS cannot consistently succeed during training, even though its robustness is similar to BC.

Visualization of robustness   Figure 3 shows which starting positions succeed during the robustness evaluation for Fetch. The green points correspond to successful episodes. We can see that both BC and BMIL succeed more frequently when starting from nearby the demonstration data (approximately
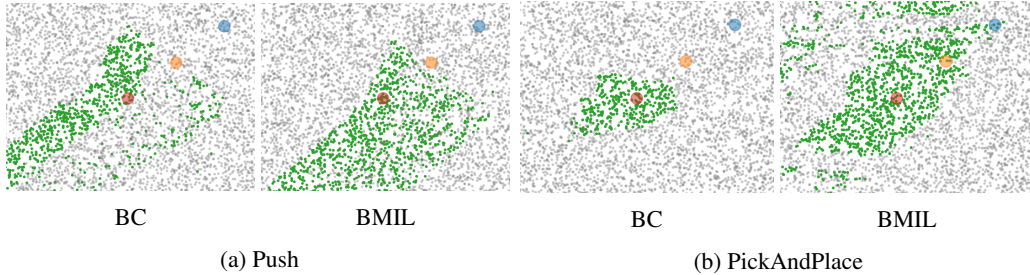
	BC	BMIL	BC	BMIL

(a) Push   (b) PickAndPlace

Figure 3: Visualization of robustness on Fetch for BC and BMIL. We vary the gripper's x, y position to evaluate robustness. The green and gray points denote successful and unsuccessful initial positions. The red, orange, and blue points denote the initial start, object, and goal during training. BMIL learns a much larger region of attraction along the path from the initial start (red) to the goal position (blue) and even succeeds in some other areas much farther away.

BC   BMIL   BC   BMIL

(a) PointRoom5x11   (b) PointCorridor7x7

Figure 4: Visualization of robustness on PointRoom5x11 and PointCorridor7x7 for BC and BMIL. The maze is discretized into a grid and 100 random states are sampled from each grid positions (each random state also adds noise to the agent's initial joint positions/velocities). Bright yellow corresponds to 100% success rate while dark purple corresponds to 0%. The regions of attraction for both BC and BMIL are similar but BMIL succeeds more often within its region of attraction.

a straight line from the start (red) to goal (blue)). However, we can see that BMIL learns a much larger region of attraction over BC and even succeeds at points that are much farther away from $\mathcal{D}_{demo}$. We hypothesize that instead of perturbing a single state within $\mathcal{D}_{demo}$ as done in VINS, learning a short reverse rollout from this state allows BMIL to learn optimal paths from states much farther away from $\mathcal{D}_{demo}$, leading to higher robustness values. Figure 4 shows a similar visualization for some Point maze environments where the agent's position is discretized into a grid. BMIL learns a region of attraction that is either slightly bigger or similar in size to that of BC but has a higher rate of success at each cell.

5.2 Additional Experiments

Forward vs Backward Dynamics We first analyze the utility of a backwards vs a forward dynamics model. On the Fetch environments, we train BMIL with a forward dynamics model $p(s' \mid s, a)$ and compare against the original backwards model $p(s, a \mid s')$. The forward model is implemented nearly identically to other n-step model-based RL algorithms (e.g. [12]), with the exception of no environment interactions. As with the backwards model, we generate rollouts from the forwards model starting from demonstrated states and train the policy on both the demonstrations and traces.

| | Robustness (%) | | | Relative to BC | | |
	BC	BMIL (Forwards)	BMIL (Backwards)	BC	BMIL (Forwards)	BMIL (Backwards)
Push (5 demos)	$12.1_{\pm 0.3}$	$12.4_{\pm 0.6}$	$14.6_{\pm 0.6}$	1	1.03	1.21
PickAndPlace (10 demos)	$4.1_{\pm 0.1}$	$4.1_{\pm 0.2}$	$17.5_{\pm 0.9}$	1	1.03	4.31

Table 2: Forwards ($p(s' \mid s, a)$) vs Backwards ($p(s, a \mid s')$) dynamics model: The forwards dynamics model performs similarly to BC and does not increase robustness.

(a) Action selection strategy
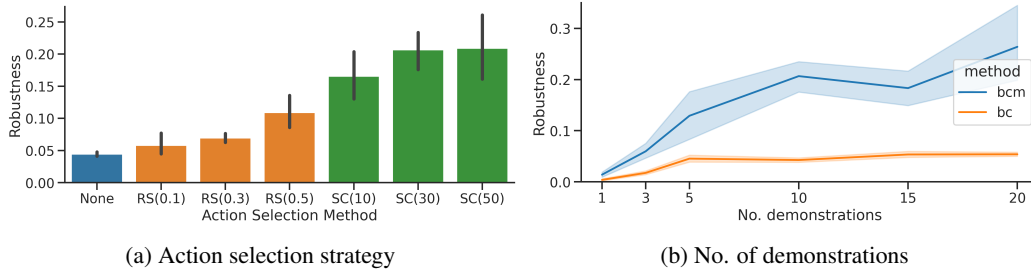

(b) No. of demonstrations

Figure 5: **(a)** Action selection strategy: effect of no perturbation (None), resampling (RS), and scaling (SC) on robustness on PickAndPlace. The numbers in the brackets indicate coefficients. We see that perturbing the first action is beneficial compared to the no perturbation (None) method and allows the backwards model to generate diverse traces. **(b)** Number of demonstrations on PickAndPlace: more demonstrations increase robustness for BC and BMIL, but BC plateaus at a much lower level.

To generate model rollouts from demonstration states, we use the action from the policy $a = \pi_\theta(s)$. The total number of parameters is kept approximately constant for the forwards and backwards models. As shown in Table 2, the forwards model offers little to no benefit over BC for both Push and PickAndPlace, suggesting that the backwards model is required to produce a robust policy.

Action selection strategy We test different action selection strategies in trace generation in Figure 5a (and Figure 10 in Appendix C.2). Compared to no perturbation (None), we see that either action selection strategy improves robustness as it can lead to more diverse trajectories unseen within the support of the demonstrations. We use the variance scaling strategy SC(30) for all Fetch experiments as it was more stable than SC(50).

Number of demonstrations We also study our method's performance with varying numbers of demonstrations. As shown in Figure 5b, both BC and BMIL improve in robustness with more demonstrations, but BC plateaus at a much lower level. On the other hand, BMIL requires slightly more (10) demonstrations than needed (3 demonstrations are sufficient for BC to succeed during training) in order to train the backwards model (Figure 11 in Appendix C.2).

Computation budget As BMIL trains both the policy and the backwards model, it requires more total gradient updates than BC. On Fetch domains, BMIL uses approximately 5x more computation than BC. We train BC for more steps to match or exceed BMIL's computation budget, as shown in Figure 6 (BC is given 1x–20x computation budget). However, more training for BC does not improve robustness and seems to have a harmful effect on robustness.

Training model first and then the policy As an offline method, BMIL does not require the backwards model to be trained in a single loop along with the policy. We can first train the model first and then train the policy. We compare training the model first and then the policy with the process outlined in Algorithm 1. We find there are no noticeable differences when using this model first approach on the Fetch domains, as seen in Table 6.
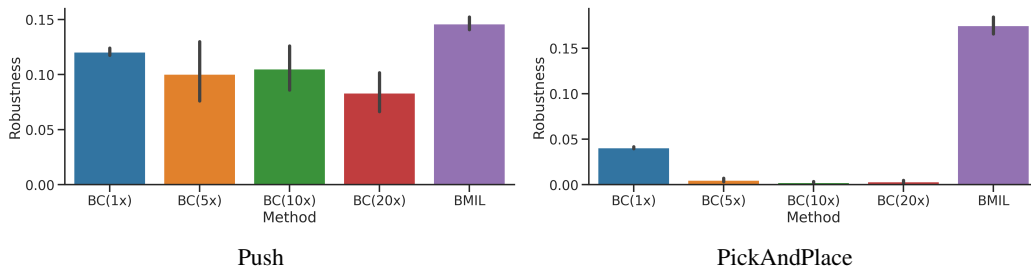

Push

PickAndPlace

Figure 6: Computation budget: we increase the number of gradient steps for BC by $1 - 20\text{x}$ for Fetch. BMIL has roughly 5 times more total gradient steps than BC(1x) due to the backwards model update. More BC gradient steps do not increase robustness.

9

6 Discussion

This work proposes a method to tackle the issue of covariate shift in imitation learning. We consider the restrictive setting where the expert is offline, where its behavior can only be inferred from demonstrations, and no access to additional environment interactions. Specifically, we show that pairing a generative backwards model with behavior cloning can allow a policy to learn a wider region of attraction around the demonstration data. By rolling out imagined traces from states within the demonstration and perturbing actions to generate diverse traces, BMIL learns a wider funnel than naive BC. Through experiments on several long-horizon, sparse-reward, continuous control domains, BMIL noticeably improves robustness when trained on a narrow set of initial start and goal states and evaluated at random starting positions.

There are many possible extensions for future work. BMIL does not necessarily preclude the use of image observations as we only assume that slightly perturbing an action will lead to new next states close to the original next state. However, to handle images, our approach likely requires an additional encoder and possibly more complex network architectures and augmentation techniques. Another interesting avenue could be to quantify how an increasing coverage of state space contained within the demonstration data affects robustness for both BC and BMIL. Finally, one could consider the setting of irrecoverable states and either resample rollouts containing such unsafe states or incorporate a measure of safety within the backwards model when generating model rollouts.

References

[1] Brenna D. Argall, Sonia Chernova, Manuela Veloso, and Brett Browning. A survey of robot learning from demonstration. *Robotics and Autonomous Systems*, 57(5):469–483, 2009. ISSN 0921-8890.

[2] Robert R. Burridge, Alfred A. Rizzi, and Daniel E. Koditschek. Sequential composition of dynamically dexterous robot behaviors. *The International Journal of Robotics Research*, 18(6): 534–555, 1999.

[3] Ashley D. Edwards, Laura Downs, and James C. Davidson. Forward-backward reinforcement learning, 2018.

[4] Justin Fu, Aviral Kumar, Ofir Nachum, George Tucker, and Sergey Levine. D4rl: Datasets for deep data-driven reinforcement learning, 2020.

[5] Scott Fujimoto, David Meger, and Doina Precup. Off-policy deep reinforcement learning without exploration. In *International Conference on Machine Learning*, pages 2052–2062, 2019.

[6] Anirudh Goyal, Philemon Brakel, William Fedus, Soumye Singhal, Timothy Lillicrap, Sergey Levine, Hugo Larochelle, and Yoshua Bengio. Recall traces: Backtracking models for efficient reinforcement learning. In *International Conference on Learning Representations*, 2019.

[7] Nathan Grinsztajn, Johan Ferret, Olivier Pietquin, Philippe Preux, and Matthieu Geist. There is no turning back: A self-supervised approach for reversibility-aware reinforcement learning. In A. Beygelzimer, Y. Dauphin, P. Liang, and J. Wortman Vaughan, editors, *Advances in Neural Information Processing Systems*, 2021.

[8] Tuomas Haarnoja, Aurick Zhou, Pieter Abbeel, and Sergey Levine. Soft actor-critic: Off-policy maximum entropy deep reinforcement learning with a stochastic actor. 2017.

[9] Todd Hester, Matej Vecerík, Olivier Pietquin, Marc Lanctot, Tom Schaul, Bilal Piot, Dan Horgan, John Quan, Andrew Sendonaris, Ian Osband, Gabriel Dulac-Arnold, John P. Agapiou, Joel Z. Leibo, and Audrunas Gruslys. Deep q-learning from demonstrations. In *AAAI*, 2018.

[10] Jonathan Ho and Stefano Ermon. Generative adversarial imitation learning. In D. Lee, M. Sugiyama, U. Luxburg, I. Guyon, and R. Garnett, editors, *Advances in Neural Information Processing Systems*, volume 29, 2016.

[11] Ahmed Hussein, Mohamed Medhat Gaber, Eyad Elyan, and Chrisina Jayne. Imitation learning: A survey of learning methods. *ACM Comput. Surv.*, 50(2), apr 2017. ISSN 0360-0300.

[12] Michael Janner, Justin Fu, Marvin Zhang, and Sergey Levine. When to trust your model: Model-based policy optimization. In *Advances in Neural Information Processing Systems*, 2019.

[13] Beomjoon Kim, Amir-massoud Farahmand, Joelle Pineau, and Doina Precup. Learning from limited demonstrations. In C. J. C. Burges, L. Bottou, M. Welling, Z. Ghahramani, and K. Q. Weinberger, editors, *Advances in Neural Information Processing Systems*, volume 26. Curran Associates, Inc., 2013.

[14] Aviral Kumar, Aurick Zhou, George Tucker, and Sergey Levine. Conservative q-learning for offline reinforcement learning. *Advances in Neural Information Processing Systems*, 33: 1179–1191, 2020.

[15] Hang Lai, Jian Shen, Weinan Zhang, and Yong Yu. Bidirectional model-based policy optimization. In Hal Daumé III and Aarti Singh, editors, *Proceedings of the 37th International Conference on Machine Learning*, volume 119 of *Proceedings of Machine Learning Research*, pages 5618–5627. PMLR, 13–18 Jul 2020.

[16] Michael Laskey, Jonathan Lee, Roy Fox, Anca D. Dragan, and Ken Goldberg. DART: noise injection for robust imitation learning. In *1st Annual Conference on Robot Learning, CoRL 2017, Mountain View, California, USA, November 13-15, 2017, Proceedings*, volume 78 of *Proceedings of Machine Learning Research*, pages 143–156. PMLR, 2017.

[17] Kimin Lee, Younggyo Seo, Seunghyun Lee, Honglak Lee, and Jinwoo Shin. Context-aware dynamics model for generalization in model-based reinforcement learning. In Hal Daumé III and Aarti Singh, editors, *Proceedings of the 37th International Conference on Machine Learning*, volume 119 of *Proceedings of Machine Learning Research*, pages 5757–5766. PMLR, 13–18 Jul 2020.

[18] Yuping Luo, Huazhe Xu, and Tengyu Ma. Learning self-correctable policies and value functions from demonstrations with negative sampling. In *International Conference on Learning Representations*, 2020.

[19] Anirudha Majumdar and Russ Tedrake. Funnel libraries for real-time robust feedback motion planning. *The International Journal of Robotics Research*, 36(8):947–982, 2017.

[20] Matthew T. Mason. The mechanics of manipulation. In *IEEE International Conference on Robotics and Automation*, 1985.

[21] Volodymyr Mnih, Koray Kavukcuoglu, David Silver, Andrei A Rusu, Joel Veness, Marc G Bellemare, Alex Graves, Martin Riedmiller, Andreas K Fidjeland, Georg Ostrovski, et al. Human-level control through deep reinforcement learning. *nature*, 518(7540):529–533, 2015.

[22] Ashvin Nair, Bob McGrew, Marcin Andrychowicz, Wojciech Zaremba, and Pieter Abbeel. Overcoming exploration in reinforcement learning with demonstrations. In *2018 IEEE International Conference on Robotics and Automation (ICRA)*, pages 6292–6299. IEEE, 2018.

[23] Suraj Nair, Mohammad Babaeizadeh, Chelsea Finn, Sergey Levine, and Vikash Kumar. Trass: Time reversal as self-supervision. In *2020 IEEE International Conference on Robotics and Automation (ICRA)*, pages 115–121, 2020.

[24] Soroush Nasiriany, Vitchyr Pong, Steven Lin, and Sergey Levine. Planning with goal-conditioned policies. In *NeurIPS*, pages 14814–14825, 2019.

[25] Takayuki Osa, Joni Pajarinen, Gerhard Neumann, J. Andrew Bagnell, Pieter Abbeel, and Jan Peters. An algorithmic perspective on imitation learning. *Foundations and Trends® in Robotics*, 7(1-2):1–179, 2018. ISSN 1935-8253.

[26] Matthias Plappert, Marcin Andrychowicz, Alex Ray, Bob McGrew, Bowen Baker, Glenn Powell, Jonas Schneider, Josh Tobin, Maciek Chociej, Peter Welinder, Vikash Kumar, and Wojciech Zaremba. Multi-goal reinforcement learning: Challenging robotics environments and request for research, 2018.

[27] Dean A. Pomerleau. Alvinn: An autonomous land vehicle in a neural network. In D. Touretzky, editor, *Advances in Neural Information Processing Systems*, volume 1. Morgan-Kaufmann, 1989.

[28] Antonin Raffin. Rl baselines3 zoo. `https://github.com/DLR-RM/rl-baselines3-zoo`, 2020.

[29] Nasim Rahaman, Steffen Wolf, Anirudh Goyal, Roman Remme, and Yoshua Bengio. Learning the arrow of time for problems in reinforcement learning. In *International Conference on Learning Representations*, 2020.

[30] Aravind Rajeswaran, Vikash Kumar, Abhishek Gupta, Giulia Vezzani, John Schulman, Emanuel Todorov, and Sergey Levine. Learning Complex Dexterous Manipulation with Deep Reinforcement Learning and Demonstrations. In *Proceedings of Robotics: Science and Systems (RSS)*, 2018.

[31] Siddharth Reddy, Anca D. Dragan, and Sergey Levine. Sqil: Imitation learning via reinforcement learning with sparse rewards. In *International Conference on Learning Representations*, 2020.

[32] Stephane Ross and Drew Bagnell. Efficient reductions for imitation learning. In Yee Whye Teh and Mike Titterington, editors, *Proceedings of the Thirteenth International Conference on Artificial Intelligence and Statistics*, volume 9 of *Proceedings of Machine Learning Research*, pages 661–668, Chia Laguna Resort, Sardinia, Italy, 13–15 May 2010. PMLR.

[33] Stephane Ross, Geoffrey Gordon, and Drew Bagnell. A reduction of imitation learning and structured prediction to no-regret online learning. In Geoffrey Gordon, David Dunson, and Miroslav Dudík, editors, *Proceedings of the Fourteenth International Conference on Artificial Intelligence and Statistics*, volume 15 of *Proceedings of Machine Learning Research*, pages 627–635, Fort Lauderdale, FL, USA, 11–13 Apr 2011. PMLR.

[34] Harsh Satija, Philip Amortila, and Joelle Pineau. Constrained Markov decision processes via backward value functions. In Hal Daumé III and Aarti Singh, editors, *Proceedings of the 37th International Conference on Machine Learning*, volume 119 of *Proceedings of Machine Learning Research*, pages 8502–8511. PMLR, 13–18 Jul 2020.

[35] Stefan Schaal et al. Learning from demonstration. *Advances in neural information processing systems*, pages 1040–1046, 1997.

[36] Julian Schrittwieser, Ioannis Antonoglou, Thomas Hubert, Karen Simonyan, Laurent Sifre, Simon Schmitt, Arthur Guez, Edward Lockhart, Demis Hassabis, Thore Graepel, et al. Mastering atari, go, chess and shogi by planning with a learned model. *Nature*, 588(7839):604–609, 2020.

[37] Yannick Schroecker, Mel Vecerik, and Jon Scholz. Generative predecessor models for sample-efficient imitation learning. In *International Conference on Learning Representations*, 2019.

[38] David Silver, Aja Huang, Christopher J. Maddison, Arthur Guez, Laurent Sifre, George van den Driessche, Julian Schrittwieser, Ioannis Antonoglou, Veda Panneershelvam, Marc Lanctot, Sander Dieleman, Dominik Grewe, John Nham, Nal Kalchbrenner, Ilya Sutskever, Timothy Lillicrap, Madeleine Leach, Koray Kavukcuoglu, Thore Graepel, and Demis Hassabis. Mastering the game of go with deep neural networks and tree search. *Nature*, 529:484–503, 2016.

[39] Wen Sun, Arun Venkatraman, Geoffrey J. Gordon, Byron Boots, and J. Andrew Bagnell. Deeply AggreVaTeD: Differentiable imitation learning for sequential prediction. In Doina Precup and Yee Whye Teh, editors, *Proceedings of the 34th International Conference on Machine Learning*, volume 70 of *Proceedings of Machine Learning Research*, pages 3309–3318. PMLR, 06–11 Aug 2017.

[40] O. Tange. Gnu parallel - the command-line power tool. *;login: The USENIX Magazine*, 36(1): 42–47, Feb 2011.

[41] Pierre Thodoroff, Audrey Durand, Joelle Pineau, and Doina Precup. Temporal regularization for markov decision process. In S. Bengio, H. Wallach, H. Larochelle, K. Grauman, N. Cesa-Bianchi, and R. Garnett, editors, *Advances in Neural Information Processing Systems*, volume 31. Curran Associates, Inc., 2018.

[42] Emanuel Todorov, Tom Erez, and Yuval Tassa. Mujoco: A physics engine for model-based control. In *2012 IEEE/RSJ International Conference on Intelligent Robots and Systems*, pages 5026–5033. IEEE, 2012.

[43] Mel Vecerik, Todd Hester, Jonathan Scholz, Fumin Wang, Olivier Pietquin, Bilal Piot, Nicolas Heess, Thomas Rothörl, Thomas Lampe, and Martin Riedmiller. Leveraging demonstrations for deep reinforcement learning on robotics problems with sparse rewards. *arXiv preprint arXiv:1707.08817*, 2017.

[44] Arun Venkatraman, Martial Hebert, and J. Andrew Bagnell. Improving multi-step prediction of learned time series models. In *Proceedings of the Twenty-Ninth AAAI Conference on Artificial Intelligence*, AAAI'15, page 3024–3030. AAAI Press, 2015. ISBN 0262511290.

[45] Jianhao Wang, Wenzhe Li, Haozhe Jiang, Guangxiang Zhu, Siyuan Li, and Chongjie Zhang. Offline reinforcement learning with reverse model-based imagination. *Advances in Neural Information Processing Systems*, 34:29420–29432, 2021.

[46] Ziyu Wang, Josh S Merel, Scott E Reed, Nando de Freitas, Gregory Wayne, and Nicolas Heess. Robust imitation of diverse behaviors. In I. Guyon, U. V. Luxburg, S. Bengio, H. Wallach, R. Fergus, S. Vishwanathan, and R. Garnett, editors, *Advances in Neural Information Processing Systems*, volume 30. Curran Associates, Inc., 2017.

[47] Keyulu Xu, Mozhi Zhang, Jingling Li, Simon S Du, Ken-ichi Kawarabayashi, and Stefanie Jegelka. How neural networks extrapolate: From feedforward to graph neural networks. *arXiv preprint arXiv:2009.11848*, 2020.

[48] Tao Yu, Cuiling Lan, Wenjun Zeng, Mingxiao Feng, Zhizheng Zhang, and Zhibo Chen. Playvirtual: Augmenting cycle-consistent virtual trajectories for reinforcement learning. In A. Beygelzimer, Y. Dauphin, P. Liang, and J. Wortman Vaughan, editors, *Advances in Neural Information Processing Systems*, 2021.

[49] Shangtong Zhang, Vivek Veeriah, and Shimon Whiteson. Learning retrospective knowledge with reverse reinforcement learning. In H. Larochelle, M. Ranzato, R. Hadsell, M. F. Balcan, and H. Lin, editors, *Advances in Neural Information Processing Systems*, volume 33, pages 19976–19987. Curran Associates, Inc., 2020.

[50] Yuke Zhu, Ziyu Wang, Josh Merel, Andrei Rusu, Tom Erez, Serkan Cabi, Saran Tunyasuvunakool, János Kramár, Raia Hadsell, Nando de Freitas, and Nicolas Heess. Reinforcement and imitation learning for diverse visuomotor skills. In *Proceedings of Robotics: Science and Systems*, Pittsburgh, Pennsylvania, June 2018.

Checklist

1. For all authors...

    (a) Do the main claims made in the abstract and introduction accurately reflect the paper's contributions and scope? [Yes]

    (b) Did you describe the limitations of your work? [Yes]

    (c) Did you discuss any potential negative societal impacts of your work? [No]

    (d) Have you read the ethics review guidelines and ensured that your paper conforms to them? [Yes]

2. If you are including theoretical results...

    (a) Did you state the full set of assumptions of all theoretical results? [N/A]

    (b) Did you include complete proofs of all theoretical results? [N/A]

3. If you ran experiments...

(a) Did you include the code, data, and instructions needed to reproduce the main experimental results (either in the supplemental material or as a URL)? [Yes] Descriptions of the implementation are provided in the main text and supplementary material and the code and data are released as a public repository.

(b) Did you specify all the training details (e.g., data splits, hyperparameters, how they were chosen)? [Yes] Briefly in Section 4, and in full in the supplementary material.

(c) Did you report error bars (e.g., with respect to the random seed after running experiments multiple times)? [Yes] See Section 5.

(d) Did you include the total amount of compute and the type of resources used (e.g., type of GPUs, internal cluster, or cloud provider)? [Yes] See supplementary material.

4. If you are using existing assets (e.g., code, data, models) or curating/releasing new assets...

   (a) If your work uses existing assets, did you cite the creators? [Yes]

   (b) Did you mention the license of the assets? [No]

   (c) Did you include any new assets either in the supplemental material or as a URL? [Yes] See Section 4.2 for the code repository URL.

   (d) Did you discuss whether and how consent was obtained from people whose data you're using/curating? [N/A]

   (e) Did you discuss whether the data you are using/curating contains personally identifiable information or offensive content? [N/A]

5. If you used crowdsourcing or conducted research with human subjects...

   (a) Did you include the full text of instructions given to participants and screenshots, if applicable? [N/A]

   (b) Did you describe any potential participant risks, with links to Institutional Review Board (IRB) approvals, if applicable? [N/A]

   (c) Did you include the estimated hourly wage paid to participants and the total amount spent on participant compensation? [N/A]
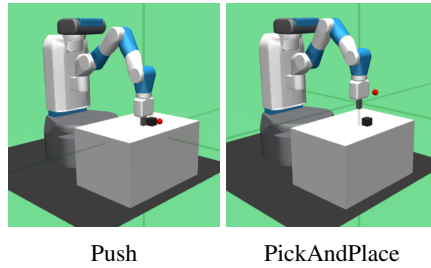
A Environments

Figure 7: Fetch robotics environments. The gripper must move the object (black) near the goal (red).

Fetch These environments from [26] involve controlling the Fetch robotic arm. We consider two tasks: "Push" and "PickAndPlace" as shown in Figure 7. The objective of "Push" is to push the object on a table towards a fixed goal position using a closed gripper. The objective of "PickAndPlace" is to pick the object by controlling the gripper and move it towards the goal. The observation space is 25-dimensional and consists of the end effector coordinates and its linear velocity, the gripper's position and velocity, and the object's pose, velocities, and its relative position/velocity to the gripper. All Fetch environments have a fixed episode length of 50 and an episode is considered successful if the object is at the goal at the end of the episode.

Maze There are 3 different maze environments of increasing difficulty and 2 different agents (Point, Ant) for each environment (c.f. Figure 8). The initial start and goal position is fixed and the objective is to control the agent to reach the goal (colored in red). The observation space is the agent's joint positions/velocities, the current timestep, and the agent's current Cartesian position. We use $dt = 0.02$ within the Mujoco [42] simulator and set the gear ratio for Ant to 10 to prevent it from falling over as in [24].

Adroit In this domain from [30], the goal is to control a 24-DoF Adroit hand to pick up a ball from the table and move it to a target location. The agent must manipulate each finger and wrist joint with dexterity to grasp the object correctly and learn the correct ball and target positions. An observation consists of hand joint angles, the object position/orientation, and the target position/orientation. We
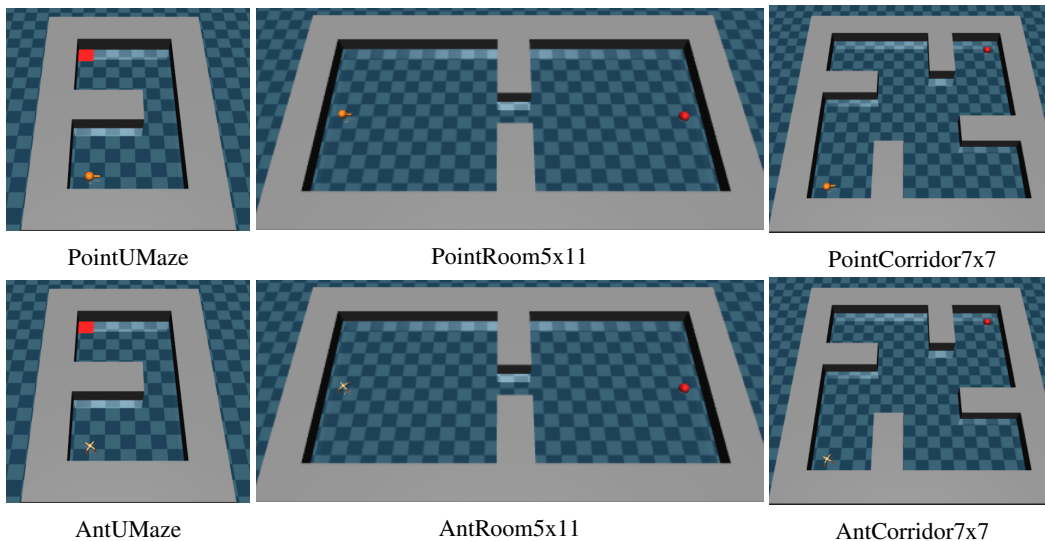

Figure 8: Maze environments. There are two agents: Point (top row) and Ant (bottom row). The agent must learn to move to the goal (red). Only the goal has a positive reward, all other states have a reward of zero.
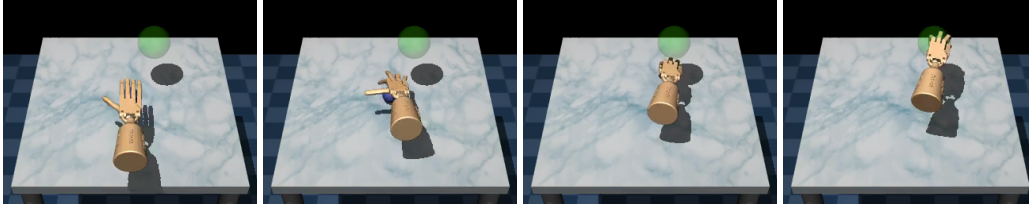
Figure 9: Adroit Relocate environment. The goal is to pick up the ball and move it to the target (green).

modify the original domain by fixing the initial `qpos` of the hand and by terminating the episode when the agent correctly solves the task.

B Experiment Details

B.1 Expert demonstrations

For the Fetch environments, we use pre-defined settings in [28] to train an expert policy. For the maze environments, we predefine a series of subgoals, and the position of the next subgoal is concatenated to the state. The reward is dense, using the negative Euclidean distance to the next subgoal and subsequent subgoals, and we use soft actor-critic [8] as the expert policy. For the Adroit environment, we use the pre-trained policy from [30].

On the Fetch domains, as each episode is of length 50, this amounts to a total of a couple of hundred training samples. We thus make 10 identical copies of each demonstration in order to stably train the policy and backwards model (we do the same for all other baselines). This has a similar effect of performing more gradient updates, but we found it to be computationally cheaper. For both Maze and Adroit environments, we use 20 demonstrations and do not repeat the demonstrations as the episodes are sufficiently long.

B.2 Hyperparameters

All hyperparameter settings for BMIL are provided in Tables 3 and 4. For all experiments, we used an internal cluster with single GPU compute nodes, with 10 virtual CPU cores and a GPU with either an NVIDIA P100 or V100.

For all methods, we use the same number of policy gradient steps for a fair comparison. For the VINS baseline, we rely on the hyperparameter settings provided in the paper for the Fetch environments and also run hyperparameter sweeps to find the best settings specific to our environments. We run longer hyperparameter sweeps for the Maze and Adroit environments.

		Fetch	Adroit
	Push	PickAndPlace	Relocate
epochs		200	600
policy updates per epoch		100	50
batch size		64	
demonstrations	5	10	20
demonstration sampling ratio p		0.5	0.8
trace horizon length	1	$1 \rightarrow 3$ $(1 \rightarrow 200)$	$1 \rightarrow 10$ $(100 \rightarrow 600)$
action selection strategy		entropy	
action selection coefficient		30	3

Table 3: Hyperparameters for Fetch and Adroit. $x \rightarrow y(a \rightarrow b)$ denotes a thresholded linear function as used in [12], implemented as $f(e) = \min\left(\max\left(x + \frac{e-a}{b-a}(y-x), x\right), y\right)$ for epoch e.

16

	Point			Ant		
	UMaze	Room5x11	Corridor7x7	UMaze	Room5x11	Corridor7x7
epochs	800			400		
policy updates per epoch	250			500		
batch size	256					
demonstrations	20					
demonstration sampling ratio p	0.8			0.95	0.9	0.95
trace horizon length	$1 \rightarrow 10$ $(100 \rightarrow 800)$			$1 \rightarrow 10$ $(100 \rightarrow 400)$		
action selection strategy	entropy					
action selection coefficient	40	1		40	10	

Table 4: Hyperparameters for Maze. $x \rightarrow y(a \rightarrow b)$ denotes a thresholded linear function.

C Results

C.1 Main results

			BC	VINS	BMIL
FETCH	Push (5 demos)		$99.8_{\pm0.5}$	$98.1_{\pm0.6}$	$99.5_{\pm0.7}$
	PickAndPlace (10 demos)		$100_{\pm0.0}$	$98.8_{\pm0.8}$	$99.2_{\pm0.8}$
MAZE	Point (20 demos)	UMaze	$95.7_{\pm1.3}$	$7.1_{\pm2.3}$	$71.6_{\pm8.0}$
		Room5x11	$96.0_{\pm1.5}$	$26.9_{\pm6.2}$	$95.7_{\pm2.6}$
		Corridor7x7	$87.2_{\pm1.7}$	$66.8_{\pm4.0}$	$90.6_{\pm2.8}$
	Ant (20 demos)	UMaze	$100_{\pm0.0}$	$39.9_{\pm5.6}$	$100_{\pm0.1}$
		Room5x11	$97.3_{\pm0.8}$	$93.5_{\pm1.3}$	$96.4_{\pm0.8}$
		Corridor7x7	$95.9_{\pm0.9}$	$88.5_{\pm1.7}$	$90.1_{\pm1.6}$
ADROIT	Relocate (20 demos)		$100_{\pm0.0}$	$96.0_{\pm1.7}$	$100_{\pm0.0}$

Table 5: Success rates during training for Fetch, Maze, and Adroit environments over $400, 100, 100$ trials, respectively. The bounds indicate 95% confidence intervals. BC and BMIL consistently solve the original task with the initial start and goal states for all environments, while the success rates for VINS fluctuate in the Maze environments.

Table 5 shows the success rates during training, on environments where the start and goal positions are unchanged. We see that both BC and BMIL achieve high success rates across all environments, while VINS does not for the Maze environments.

C.2 Additional Experiments

For all additional experiments on the Fetch domains, we use 100 trials for each method. The error bars or shaded regions denote 95% confidence intervals.
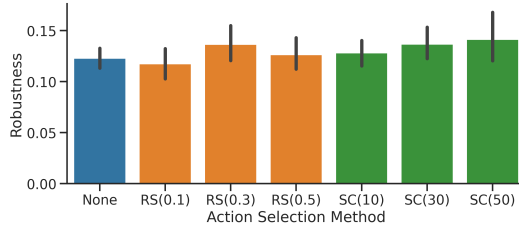

Figure 10: Action selection strategy on Push. We see a similar trend as in PickAndPlace, in that perturbing the action increases robustness over None.

Figure 10 shows the robustness of different action selection strategies on Fetch-Push. Here we see that all action selection strategies generally perform similarly, with possibly RS(0.3) and SC(50) a slight edge over the no strategy (None), though the error bars are fairly large.
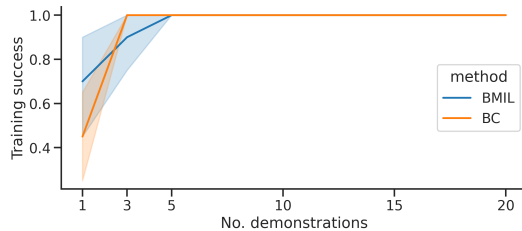

Figure 11: Number of demonstrations: training success rates on PickAndPlace.

Figure 11 shows the success rates during training with a varying number of demonstrations on Fetch-PickAndPlace. We see that 3 demonstrations are sufficient for BC to achieve a 100% success rate on the original start and goal positions. However, BMIL requires at least 5 demonstrations to attain the same level of performance, as the backwards model requires at least a certain number of samples to train in a stable manner. We use 10 demonstrations in our experiments.

	Robustness (%)			Relative to BC		
	BC	BMIL	BMIL (model first)	BC	BMIL	BMIL (model first)
Push (5 demos)	$12.1_{\pm 0.3}$	$14.6_{\pm 0.6}$	$13.2_{\pm 1.0}$	1	1.21	1.09
PickAndPlace (10 demos)	$4.1_{\pm 0.1}$	$17.5_{\pm 0.9}$	$19.9_{\pm 2.4}$	1	4.31	4.85

Table 6: Training the backwards model first and then the policy produces similar results as training them together (BMIL).

Table 6 shows the results of training the backwards model first compared to BMIL which trains both the model and the policy in the same training loop. We find similar robustness values, where training the model first produces slightly lower values on Push and slightly higher values on PickAndPlace.